Myosin 5a controls insulin granule recruitment during late phase secretion

Running title: Recruitment of insulin granules by myosin 5a

Rosita Ivarsson[1], Xingjun Jing[1], Laurent Waselle[2], Romano Regazzi[2] and Erik Renström[1,3].

1: Department of Experimental Medical Science, Lund University, Lund, Sweden

2: Département de Biologie Cellulaire et de Morphologie, University of Lausanne, Lausanne, Switzerland

3: Corresponding author: Erik Renström, Dept.Experimental Medical Science, Tornav. 10, BMC B11, 221 84 LUND, Sweden.

Phone: +46-46-2220639, Fax +46-46-2227763

Email: erik.renstrom@med.lu.se

Abstract

We have examined the importance of the actin-based molecular motor myosin 5a for insulin granule transport and insulin secretion. Expression of myosin 5a was down-regulated in clonal INS-1E cells using RNAinterference. Stimulated hormone secretion was reduced by 46% and single-cell exocytosis, measured by capacitance recordings, was inhibited by 42% after silencing. Silencing of Slac-2c/MYRIP, which links insulin granules to myosin 5a, resulted in similar inhibition of single-cell exocytosis. Antibody inhibition of the myosin 5a-Slac-2c/MYRIP interaction significantly reduced the recruitment of insulin granules for release. The pool of releasable granules independent of myosin 5a activity was estimated to ~550 granules.

TIRF microscopy was then applied to directly investigate granule recruitment to the plasma membrane. Silencing of myosin 5a inhibited granule recruitment during late phase of insulin secretion. In conclusion we propose a model where insulin granules are transported through the actin network via both myosin 5a-mediated transport and via passive diffusion, with the former playing the major role during stimulatory conditions.

INTRODUCTION

Insulin is stored in secretory granules that are released from pancreatic beta-cells by Ca^{2+}-dependent exocytosis (1). When blood glucose is elevated insulin is secreted in a biphasic manner, consisting of a first rapid phase lasting 5-10 minutes, followed by a sustained second phase of secretion. Insulin granules released during the first phase are already situated at the plasma membrane (2, 3), whereas granules released during the second phase are recruited to the cell periphery (4). In the cell center, granules are transported along microtubules mediated by conventional kinesins (5, 6). At the cell periphery, however, the transport of granules is dependent on the actin network. The nature of this transport is unclear. Myosin 5a is an actin-based molecular motor that has been demonstrated to be involved in the transport of secretory granules in several cell systems (7). Recently, an important role for myosin 5a for insulin granule transport and release was demonstrated in the mouse insulinoma cell line MIN6 (8). Briefly described, myosin 5a is a two headed motor consisting of two identical heavy chains and multiple light chains. The heavy chain binds to actin via its N-terminal domain and to the cargo via its C-terminal domain (9). Using the two head domains the motorprotein can walk along the actin filaments in 37 nm large steps at a speed of about 400 nm/s (10, 11). The importance of myosin 5a for organelle transport is

evident in the dilute mice (12), where a mutation of myosin 5a leads to a non-functioning transfer of pigment granules and results in a dilute fur color. In humans, mutations of myosin 5a causes Griscelli syndrom, a rare disease characterized by partial albinism and immunodeficiency (13). The interaction between myosin 5a and insulin granules is likely to be mediated via Rab 27a and Slac-2c/MYRIP. Both Rab 27a and Slac-2c/MYRIP are associated to insulin granules (14) and Slac-2c/MYRIP has been shown to bind myosin 5a in other secretory cells (15). Interestingly, it was recently reported that mice with a naturally occurring mutation in Rab27A (*Ashen* mice) exhibit defective glucose-stimulated insulin secretion, as well as impaired insulin granule transport (16).

Here, we have extended on earlier reports by specifically adressing the role of myosin 5a in the recruitment of new insulin granules to cell periphery during late phase insulin secretion. The expression of myosin 5a was silenced in insulin-secreting cells using RNAinterference (RNAi) to study the effect on single-cell exocytosis, hormone secretion and granule recruitment. We demonstrate that insulin secretion is dependent on myosin 5a activity, in particular during stimulatory conditions. We also show that myosin 5a is involved in the recruitment of granules to the plasma membrane during second phase of insulin secretion.

RESULTS

Role of the actin cortex in insulin release

The localization of the actin filament network in INS-1 cells was studied by phalloidin stainings (Fig. 1a). Actin filaments were confined to a thin layer beneath the plasma membrane. The role of the actin filament network for insulin exocytosis

was investigated by capacitance recordings in cells treated with the actin polymerisation inhibitor cytochalasin D. This compound had an effect on the voltage-gated Ca^{2+} currents, and we therefore evoked exocytosis by intracellular dialysis of a Ca^{2+}/EGTA-containing pipette solution ($[Ca^{2+}]_{i\ free}$ 1.5 μM) using the standard whole-cell configuration of the patch-clamp technique. Cell capacitance started to increase immediately after establishment of the standard whole-cell configuration. In untreated cells, the rate of capacitance increase during the first minute was 13±4 fF/s (n=15). In cytochalasin D-treated cells (10 μM for >15 min), exocytosis was accelerated by >170% ($p<0.05$ vs. control, n=11, Fig. 1b). Similar results were also obtained with the actin inhibitor latrunculin B (not shown).

Expression and cellular localisation of myosin 5a

Myosin 5a expression in INS-1E cells was demonstrated by immunoblotting (Fig. 2a). The localisation of myosin 5a in INS-1E cells was studied by confocal immunocytochemistry (Fig 2b). Myosin 5a exhibited a diffuse granular pattern throughout the cytoplasm, whereas insulin showed a more distinct punctuate pattern. Partial co-localisation was observed for myosin 5a and insulin.

Silencing of myosin 5a using RNAi

Due to the low transfection rate in INS-1E cells (~10%), we investigated the myosin 5a silencing effect in the COS-7 cell line. COS-7 cells were transfected with the different silencing vectors together with a myosin 5a expressing vector and the silencing effeciency was measured by immunoblotting. Compared to control cells, transfected with empty pSuper, the expression of myosin 5a was reduced by 65% in silMyo5a1 transfected COS-7 cells (Fig. 3a). The expression of non-muscle myosin

2a, another unconventional myosin, was not affected (Fig. 3a), demonstrating a specific silencing effect of myosin 5a.

Myosin 5a silencing inhibits hormone secretion

To study the effect of protein silencing on hormone secretion in transfected cells we applied a growth hormone (GH) assay as previously described (14, 17). Briefly, this method is based on the co-expression of siRNA and GH in the transfected cells. Since only transfected cells will express GH, which is localized and secreted together with insulin, secretion from non-transfected cells will not influence the measurements. Silencing of myosin 5a had no effect on basal GH secretion (5 mM K^+, 0 glucose). In control cells 6.5 ± 0.7% of the total GH content was released and 6.4 ± 1.1% was released from RNAi treated cells (n.s., n=11 and 10, respectively; Fig. 3b). When cells were stimulated (80 mM K^+, 20 mM glucose, 1 mM IBMX and 1 μM forskolin) the response was elevated by 174 ± 28% (17.7 ± 2.4% of total GH content) in control cells compared to only 95 ± 27% (12.5 ± 2.0% of total GH content) in RNAi treated cells ($p<0,05$, n=11 and 10, respectively; Fig 3b). These data show that myosin 5a is important for secretion under stimulatory conditions but not at basal.

Myosin 5a inhibits single-cell exocytosis

Cell-capacitance recordings were performed to study exocytosis and granule mobilisation in single-cells with a high time resolution. Transfected cells were identified by EGFP expression and exocytosis was triggered by application of a train of ten depolarisating pulses from –70 to 0 mV. Silencing of myosin 5a resulted in 42% reduction of exocytosis during the complete train (pulse 1-10) compared to cells transfected with empty pSuperEGFP (Fig. 4a; from 433 ± 53 fF to 250 ± 43 fF;

p<0.05; n=7). Silencing of myosin 5a showed a symmetrical inhibition of ~ 42% on both the capacitance increase from the first pulse in the train (from 115 ± 17 fF to 67 ± 12 fF; P<0.05; n=7), representing release of granules belonging to a readily releasable pool (RRP), and from the latter part of the train (pulse 2-10, from 319 ± 50 to 183 ± 38; P=0.05; n=7), representing mobilisation of granules to the RRP.

Slac-2c/MYRIP and myosin 5a silencing have similar effects on exocytosis

Silencing of Slac-2c/MYRIP resulted in a similar inhibitory effect on exocytosis as silencing of myosin 5a. In Slac-2c/MYRIP-silenced cells the total cell capacitance increase in response to a train of depolarisations was reduced by 41% compared to the control cells (Fig. 4b; 429 ± 64 fF and 252 ± 49 fF, p <0.05; n=8 and n=10, respectively).

It was verified that the inhibitory effects of myosin 5a- and Slac-2c/MYRIP silencing were not associated with a reduction in voltage-dependent Ca^{2+}-influx. Average integrated Ca^{2+}-currents in myosin 5a- and Slac-2c/MYRIP-silenced cells measured 95% and 99%, respectively, when compared with control cells.

Antibody inhibition of myosin 5a function

To further investigate the effects of myosin 5a inhibition on exocytosis we performed antibody infusion experiments. In contrast to the RNAi technique, this method is suitable to study acute effects of myosin 5a inhibition. To this end an antibody raised against a 22 amino acid peptide, corresponding to the cargo-interacting site in the tail domain of myosin 5a (18) was included in the intracellular patch solution. This antibosy can be predicted to block the interaction between myosin 5a and Slac-

2c/MYRIP. After allowing the antibody to wash into the cell for two minutes the first train of depolarisations was applied, followed by new trains applied at one minute intervals. The first train of depolarisations resulted in 32% reduction of exocytosis (222 ± 28 fF for anti-myosin 5a compared to 328 ± 80 fF for control, p=n.s., n=5 for both groups). The following trains resulted in a use-dependent increasing inhibitory effect on exocytosis, which after six minutes reached a steady-state level. The capacitance increase in response to the fifth train of stimulation (applied after 6 minutes) amounted to only 32 ± 24 fF (i.e. 14% of the first train) compared to 268 ± 67 fF (i.e. 82% of the first train) in control cells ($p<0.01$, n=5 for both groups, Fig. 5). From these data a least-squares fit to the first order exponential decay function was applied, showing that a pool of granules corresponding to a ~460 fF increase in cell capacitance can be released independently of myosin 5a-cargo interaction.

Imaging of insulin granule recruitment to the plasma membrane during glucose stimulation

Overall granule mobility was studied by live confocal imaging of labeled insulin granules. As expected, no difference was observed after silencing of myosin 5a since this method primarily visualizes microtubule-based granule movements in the cell center (data not shown). To investigate actin-based granule movements we instead performed TIRF microscopy. Using this method we explored whether a difference in the recruitment of new granules to the plasma membrane could be observed after myosin 5a silencing compared to control cells during 20 minutes of glucose stimulation. The number of docked granules, seen as white dots (Fig. 6a) was calculated every second minute and normalized to the number of granules observed in the first image in the experiment. Initailly the number of docked granules decreased in

both control and myosin 5a silenced cells. After 12 minutes the average number of granules stabilized at a level of ~ 40% of the initial number of docked granules in the control cells, whereas in myosin 5a silenced cells the number of docked granules decreased throughout the experiment. For example, after 20 minutes of glucose stimulation the amount of docked granules was 19 ± 4% of initial in myosin 5a silenced cells compared to 36 ± 3% of initial in control cells ($p<0.01$; n=8, Fig. 6b).

DISCUSSION

Dual role of the actin network

The role of the actin network in insulin secretion is unsettled. Disruption of the actin network stimulates insulin secretion (Fig. 1b) and the actin network has therefore been suggested to function as a barrier hindering insulin granules to reach the plasma membrane by diffusion (19). In addition, actin filaments have been suggested to provide tracks for secretory granules (20). In line with this, Varadi et al recently demonstrated that insulin granules interact with myosin 5a (8) and that the motorprotein indeed is involved in insulin granule delivery at the plasma membrane. Here, we have extended on these findings by specifically addressing the importance of myosin 5a for sustained late phase of glucose-evoked insulin secretion. Accumulating evidence therefore indicate of a dual action of the actin network for insulin secretion, i.e. that the cortical actin web both acts as a diffusion barrier as well as a track for insulin granule transport to the release sites at the plasma membrane.

Myosin 5a in basal secretion

Silencing of myosin 5a resulted in impaired hormone secretion during stimulatory conditions but had no impact on basal secretion (Fig. 3b). This indicates that insulin

granules can be recruitment in a non myosin 5a-dependent process and that this process fulfills the recruitment necessary for basal secretion. We have previously demonstrated the importance of random diffusive movements in insulin secretion (5) and we speculate that a fraction of insulin granules can reach the plasma membrane by diffusion through the actin network. During stimulatory conditions, however, it is clear that an active transport is necessary to fulfill the accelerated granule recruitment and we demonstrate the importance of myosin 5a in this process.

Myosin 5a in regulated secretion

First phase of insulin secretion represents release of insulin from the readily releasable pool (RRP), that consists of granules already docked to the plasma membrane (2-4), whereas, for the second phase granules are recruited to the plasma membrane during the stimulation. The number of granules situated close to the plasma membrane has been shown to exceed the number of granules released during several hours of stimulated insulin secretion (21), however studies in primary rat beta-cells and MIN6 cells using TIRF microscopy show that granules released during second phase of insulin secretion are newcomers that are actively transported to the plasma membrane (4, 22). Our data from TIRF experiments (Fig. 6) support that granules realesed during second phase of secretion are newcomers and that myosin 5a is involved in this recruitment.

As mentioned above it was evident that myosin 5a activity was necessary during stimulatory conditions to fulfill the recruitment of new granules to the plasma membrane. The same conclusion could be drawn from the capacitance recordings, where exocytosis was studied both after silencing of myosin 5a, using the RNAi

technique, as well as after acute inhibition of myosin 5a by intracellular infusion of an inhibitory antibody. Both approaches resulted in significant inhibition of exocytosis already after the first train of depolarisations (42% and 32%, respectively). This indicates that the pool of releasable granules, is instable and requires the continous refilling by a myosin 5a dependent process. Moreover, when stimulating with repeated trains of depolarisations the inhibitory effect became stronger until it reached a steady state level after ~5 trains (Fig. 5b). From this we estimated that a pool of granules corresponding to an increase in capacitance of 460 fF could be released independent of myosin 5a activity. From electromicrographs of large dense-core vesicles in INS-1 cells the average diameter of an insulin granule is 171 ± 3 nm, corresponding to a capacitance increase of 0.83 fF /granule (23). The number of granules released independently of myosin 5a activity can then be estimated to ~550 granules.

Myosin 5a and its interaction partners

Myosin 5a is known to interact with several other proteins regulating exocytosis, e.g. Rab27a and Slac-2c/MYRIP. Interestingly, recently a vital role for Rab 27a in insulin granule docking to the plasma membrane was reported in *Ashen* mice that carry a naturally occurring mutation in the Rab27a gene. Furthermore, *Ashen* mice also exhibit impaired glucose-evoked phasic insulin secretion and glucose intolerance (16). It is tempting to speculate that impaired insulin granule docking in *Ashen* mice is due to the suppressed function of Myo 5a.

Another interaction partner is Slac-2c/MYRIP. Silencing of myosin 5a and Slac-2c/MYRIP had very similar inhibitory effect on single-cell exocytosis. This supports a

role of these proteins in the recruitment of new granules for secretion and further that the function of myosin 5a for granule recruitment is mediated via the interaction with Slac-2c/MYRIP. The exact function of Slac-2c/MYRIP is unclear. In agreement with our results Waselle et al, 2003 found that Slac-2c/MYRIP silencing impairs exocytosis. It is of great interest that Slac-2c/MYRIP in addition to a myosin 5a-binding site also has a direct actin-binding site. Overexpression of Slac-2c/MYRIP leads to impaired granule mobility and reduces hormone secretion in PC-12 cells (24), however expression of a Slac-2c/MYRIP construct lacking the actin binding domain also lead to impaired hormone secretion but increased mobility (24). We speculate that the association of insulin granules to the actin network might function as a docking site for the granules and that myosin 5a mediated translocation can only occur after detachment of Slac-2c/MYRIP from the cytoskeleton. What regulates the Slac-2c/MYRIP-actin interaction remains to discovered, but it was recently found that Slac-2c/MYRIP has multiple PEST sites and that especially PEST sites in the actin-binding C-terminal end of the protein are sensitive to calpains (25). Calpain 10 is a calcium-sensitive protease that has been associated with type-2 diabetes in genetic linkage analysis (26).

The direct regulators of myosin 5a-dependent secretory granule transport is unclear. Several mechanisms have been suggested in other cell types, such as regulation of cargo binding by calcium/calmodulin-dependent protein kinase II (27), regulation of motor activity by MLCK (28), and regulation of cargo detachment by calpains (29). All of these mechanisms are calcium dependent and would therefore be activated in parallel with calcium-evoked exocytosis in insulin secreting beta-cells.

We conclude that insulin granules are recruited to the plasma membrane by myosin 5a-dependent transport along actin filaments or by passive diffusion through the actin network. During stimulatory conditions active transport of granules is required to fulfill the necessary recruitment. The importance of myosin 5a-mediated transport is evident ~12 minutes after the onset of stimulation, which coincides with second phase of insulin secretion.

MATERIALS AND METHODS

Cell culture

Rat insulinoma INS-1 cells (passage 92-110); (30) and INS-1E cells (passage 52-75) were cultured in RPMI 1640 medium (11 mM glucose; Gibco BRL, Invitrogen, Stockholm, Sweden) supplemented with 10% fetal calf serum, streptomycin (100 μg/ml), penicillin (100 μg/ml) and 2-mercaptoethanol (50 μM) at 37°C and 5% CO_2. INS-1E cells is a subclone of INS-1, which is more glucose-responsive and stable in culture (31). COS-7 cells were cultured in Dulbecco's MEM (Gibco) supplemented with 10% fetal calf serum, nonessential amino acids, streptomycin (100 μg/ml) and penicillin (100 μg/ml).

Immunocytochemistry

For immunocytochemistry cells were plated on glass coverslips and fixed in 3% parafolmardehyde and permeabilized with PBS+0.1% triton X-100. For staining of actin filaments, INS-1 cells were incubated with the fluorescent f-actin probe Alexa Fluor 488-phalloidin (Molecular Probes, Leiden, The Netherlands). A methanolic stock solution with ≈6.6 μM of the probe, and 1% BSA was made and 5 μL of this stock solution was mixed with 200 μL PBS and added to each coverslip to be stained.

Confocal images were obtained with a Zeiss LSM 5 Pascal Microscope (Zeiss, Jena, Germany). Fluorescence was excited using the 488 nm line of an argon laser and emission was collected using a 505 nm long pass filter. To evaluate co-localisation of myosin 5a and insulin, INS-1E cells were fixed and permeabilized as above followed by incubation in PBS+5% normal donkey serum. The cells were then stained with a polyclonal anti-myosin 5a antibody (dilution 1:200, LF-18, Sigma-Aldrich, Saint Louis, MO, USA) and an anti-insulin antibody (dilution 1:500, B 65-1, EuroDiagnostica, Arnhem, The Netherlands) followed by Cy3-conjugated anti-rabbit (for myosin 5a) and Cy 5-conjugated anti-guinea pig (for insulin) secondary antibodies (both diluted 1:150, Pierce, Rockford, IL, USA). Cy3 fluorophores were excited with a 543 nm HeNe laser and emission collected using a 560-615 band pass filter. Cy5 fluorophores were excited with a 633 nm HeNe laser and emission collected using a 650 nm long pass filter.

Design of RNAinterference vectors for silencing of myosin 5a

The pSuper system (Oligoengine, Seattle, WA, USA) was used for target-specific protein silencing using expression of short interfering RNA (siRNA). Three 19 nucleotide (nt) sequences specific for rat myosin 5a (SilMyo5a1: nt 95-113: GCCTGGAGATAAAGTGCTC, SilMyo5a2: nt 107-125: AGTGCTCCTGCTTCA-CCTT and SilMyo5a3: nt 213-231: AATGACCTCACAGCCCTCA, positions counted from the start codon) were selected and three 64 basepair oligos were designed according to instructions from Oligoengine. The oligos were inserted into the pSuper vector and the correct positions were confirmed by sequencing. The silencing effect of the three constructs were tested by immunoblotting (see below). The most effective construct (SilMyo5a1) was selected for further experiments. For

co-expression of siRNA and EGFP, the CMV promotor and EGFP cDNA was inserted into pSuper using the Sac1 and Pst1 restriction sites in front of the H1-promotor (pSuperEGFP). For silencing of Slac-2c/MYRIP (SilSlac-2cEGFP) the same oligo as used in Waselle et al., 2003 (RNAi/2Slac2c:nt 2339-2357 of human Slac2c/MYRIP) was cloned into pSuperEGFP. In all experiments empty pSuper or empty pSuperEGFP were used as control vector.

Capacitance recordings

Exocytosis was measured by capacitance recordings using the whole-cell configuration of the patch-clamp technique. In figure 1, INS-1 cells were cultured in Corning Petri dishes and pretreated with the actin-disrupting agent cytochalasin D (10 μM, Sigma-Aldrich) for 15 min. Patch electrodes were made from borosilicate glass capillaries coated with Sylgard, fire-polished and filled with intracellular pipette solution. Exocytosis was elicited by wash in of the intracellular pipette solution (in mM: 125 K-glutamate, 10 NaCl, 10 KCl, 1 MgCl2, 5 HEPES, 3 Mg-ATP, 0.1 cAMP, 10 EGTA, 9 $CaCl_2$, pH 7.2 with KOH), with a free intracellular $[Ca^{2+}]_i$ of ≈1.5 μM, estimated using the binding constants of Martell and Smith (1974). The cells were continuously perfused with pre-heated (34ºC) extracellular (EC) buffer (in mM: 138 NaCl, 5.6 KCl, 1.2 $MgCl_2$, 2.6 $CaCl_2$, 5 HEPES, pH 7.4 with NaOH) supplemented with 3 mM glucose. Exocytosis was measured as the rate of capacitance increase using an EPC9 amplifier (HEKA Electronics, Lambrecht/Pfalz, Germany) in conjunction with the HEKA pulse software suite.

For the capacitance recordings on myosin 5a- and Slac-2c/MYRIP-silenced cells (Fig. 4), INS-1E cells were transfected with SilMyo5a1EGFP, SilSlac-2cEGFP or

pSuperEGFP. For these experiments exocytosis was stimulated using trains of ten 300 ms voltage-clamp depolarisations from –70 to 0 mV. A shorter pulse duration was chosen compared to the antibody infusion experiments (see below) to avoid compensatory endocytotic responses. To resolve the inward voltage-activated Ca^{2+}-currents the intracellular pipette solution consisted of (mM) 125 Cs-glutamate, 10 NaCl, 10 CsCl, 1 $MgCl_2$, 5 HEPES, 3 Mg-ATP, 0.1 cAMP (pH 7.2 with CsOH) and in the EC buffer 20 mM of NaCl was equimolarly replaced by tetraethylammonium chloride (TEA-Cl).

For the antibody infusion experiments (Fig. 5) non-transfected INS-1 cells were used. The solutions were the same as for the silencing experiments (Fig. 4) except for that the intracellular pipette solution was supplemented with an antibody towards the C-terminal end of myosin 5a, previously characterized in (18) (dilution 1: 250, the antibody was a kind gift from J. Leonard, Worcester, PA, USA). For the controls non immunized mouse IgG (5 μg/ml) was added to the pipette solution. After whole-cell establishment the antibody was allowed to wash into the cell for 2 minutes before trains of ten 500 ms depolarisations from –70 mV to 0 mV were applied. The trains were repeated at 1 min intervals until no exocytosis was observed.

Immunoblotting

The silencing effect of myosin 5a RNAi was analysed by immunoblotting. COS-7 cells were transfected with both the different pSuper constructs and a myosin 5a expressing vector using Effectene transfection reagent (Qiagen, Hilden, Germany). After 72 h the cells were homogenized and equal amounts of proteins were separated on a 7.5% polyacrylamide gel followed by blotting onto a nitrocellulose membrane.

Myosin 5a expression was identified using a polyclonal anti-myosin 5a antibody (LF-18, dilution 1:500) and a horseradish peroxidase-conjugated secondary antibody. As a control for the specificity of the myosin 5a siRNA, non-muscle myosin 2a expression was investigated using a polyclonal antibody against non-muscle myosin 2a heavy chain (dilution: 1:5000 Babco, Richmond, CA, USA) and the same secondary antibody as for myosin 5a. Chemiluminiscence were detected using SuperSignal ® West Pico Chemiluminiscent Substrate (Pierce Biotechnology, Rockford, IL, USA) in a Fluo Max detection system (BioRad, Hercules, CA, USA). Quantification of protein expression was made using Quantity One software (BioRad).

Growth hormone secretion assay

INS-1E cells were plated in 24-well dish (300 000 cells/well) and co-transfected with 0,2 μg SilMyo5a1 vector or empty pSuper and 0,2 μg human Growth hormone (GH) expressing vector (32) using Effectene transfection reagent. After 72 h cells were washed and preincubated for 30 minutes at 37ºC in: (mM) 20 HEPES, 128 NaCl, 5 KCl, 1 $MgCl_2$, 2.7 $CaCl_2$, 0.1% BSA (pH 7.4). The cells were then incubated for 45 min in either the same buffer (basal secretion) or in: (mM) 20 HEPES, 53 NaCl, 80 KCl, 1 $MgCl_2$, 2.7 $CaCl_2$, 0.1% BSA, 20 glucose, 1 IBMX, 1 μM Forskolin (pH 7.4) (stimulated secretion). After collection of secretion samples the cells were harvested in PBS+0.1% triton X-100, sonicated and centrifuged to remove cell debris. Analysis of GH content in secretion samples and cell homogenates were made with GH ELISA (Roche Diagnostics, Stockholm, Sweden). Data are presented as ratio secreted GH to total GH content/well, to compensate for variations in transfection efficiency.

TIRF microscopy

INS-1E cells were plated on glass coverslips and co-transfected with SilMyo5a1 or empty pSuper and IAPP-emerald (33) to visualize insulin granules. After 72 h fluorescent granules close to the plasma membrane (within ~ 300 nm) were visualized using a Total Internal Reflection Module from TILL Photonics GmbH (Gräfelfing, Germany) together with an inverted Zeiss Axiovert 200 microscope equipped with a Zeiss Alpha-Plan Fluar 100x/1.45 oil objective. IAPP-emerald fluorescence was excited at 488 nm using a Spectraphysics 385F laser and images were captured using a CoolSNAP HQ digital camera (Photometrics, Tucson, AZ, USA). Image acquisition and analysis were made using MetaMorph (version 6, Universal Imaging Corporation, Downington, USA). Cells were perfused with pre-heated EC buffer (in mM: 138 NaCl, 5.6 KCl, 1.2 $MgCl_2$, 2.6 $CaCl_2$, 5 HEPES, pH 7.4 with NaOH) without glucose for 15 min. Images were collected every second minute from 0 to 20 minutes after addition of EC buffer with 20 mM glucose. The number of docked granules were counted in each image and related to the number of docked granules at the onset of the experiment.

Data analysis

Data are presented as mean values ± S.E.M. The statistical significance of difference between two groups were evaluated using two-tailed unpaired Student's t-test.

Acknowledgements

We thank Dr C.B. Wollheim, Geneva, Switzerland for kindly providing INS-1E cells, and Ulrika Fransson, Lund University for sharing constructs and help with molecular

cloning. We also thank Dr. P. Rorsman for generously providing imaging equipment. R.I. was supported by The Royal Physiographic Society in Lund. E.R. was supported by grants from the Swedish Research Council (grants no. 12234, 13509), The Royal Physiographic Society in Lund, The European Foundation for the Study of Diabetes, The Hain Foundation, The Albert Påhlsson Foundation, The NovoNordisk Foundation, The Swedish Diabetes Association and the Crafoord Foundation. R. R. was supported by the Swiss National Fund (grant no. 3200B0-101746).

References

1. Wollheim CB, Sharp GW. Regulation of insulin release by calcium. Physiol Rev 1981;61(4):914-73.
2. Daniel S, Noda M, Straub SG, Sharp GW. Identification of the docked granule pool responsible for the first phase of glucose-stimulated insulin secretion. Diabetes 1999;48(9):1686-90.
3. Barg S, Eliasson L, Renstrom E, Rorsman P. A subset of 50 secretory granules in close contact with L-type Ca2+ channels accounts for first-phase insulin secretion in mouse beta-cells. Diabetes 2002;51 Suppl 1:S74-82.
4. Ohara-Imaizumi M, Nakamichi Y, Tanaka T, Ishida H, Nagamatsu S. Imaging exocytosis of single insulin secretory granules with evanescent wave microscopy: distinct behavior of granule motion in biphasic insulin release. J Biol Chem 2002;277(6):3805-8.
5. Ivarsson R, Obermuller S, Rutter GA, Galvanovskis J, Renstrom E. Temperature-Sensitive Random Insulin Granule Diffusion is a Prerequisite for Recruiting Granules for Release. Traffic 2004;5(10):750-62.
6. Varadi A, Ainscow EK, Allan VJ, Rutter GA. Involvement of conventional kinesin in glucose-stimulated secretory granule movements and exocytosis in clonal pancreatic beta-cells. J Cell Sci 2002;115(Pt 21):4177-89.
7. Langford GM. Myosin-V, a versatile motor for short-range vesicle transport. Traffic 2002;3(12):859-65.
8. Varadi A, Tsuboi T, Rutter GA. Myosin Va Transports Dense Core Secretory Vesicles in Pancreatic MIN6 {beta}-Cells. Mol Biol Cell 2005.
9. Reck-Peterson SL, Provance DW, Jr., Mooseker MS, Mercer JA. Class V myosins. Biochim Biophys Acta 2000;1496(1):36-51.
10. Yildiz A, Forkey JN, McKinney SA, Ha T, Goldman YE, Selvin PR. Myosin V walks hand-over-hand: single fluorophore imaging with 1.5-nm localization. Science 2003;300(5628):2061-5.
11. Cheney RE, O'Shea MK, Heuser JE, Coelho MV, Wolenski JS, Espreafico EM, et al. Brain myosin-V is a two-headed unconventional myosin with motor activity. Cell 1993;75(1):13-23.

12. Mercer JA, Seperack PK, Strobel MC, Copeland NG, Jenkins NA. Novel myosin heavy chain encoded by murine dilute coat colour locus. Nature 1991;349(6311):709-13.
13. Menasche G, Ho CH, Sanal O, Feldmann J, Tezcan I, Ersoy F, et al. Griscelli syndrome restricted to hypopigmentation results from a melanophilin defect (GS3) or a MYO5A F-exon deletion (GS1). J Clin Invest 2003;112(3):450-6.
14. Waselle L, Coppola T, Fukuda M, Iezzi M, El-Amraoui A, Petit C, et al. Involvement of the Rab27 binding protein Slac2c/MyRIP in insulin exocytosis. Mol Biol Cell 2003;14(10):4103-13.
15. Fukuda M, Kuroda TS. Slac2-c (synaptotagmin-like protein homologue lacking C2 domains-c), a novel linker protein that interacts with Rab27, myosin Va/VIIa, and actin. J Biol Chem 2002;277(45):43096-103.
16. Kasai K, Ohara-Imaizumi M, Takahashi N, Mizutani S, Zhao S, Kikuta T, et al. Rab27a mediates the tight docking of insulin granules onto the plasma membrane during glucose stimulation. J Clin Invest 2005;115(2):388-96.
17. Iezzi M, Regazzi R, Wollheim CB. The Rab3-interacting molecule RIM is expressed in pancreatic beta-cells and is implicated in insulin exocytosis. FEBS Lett 2000;474(1):66-70.
18. Stachelek SJ, Kowalik TF, Farwell AP, Leonard JL. Myosin V plays an essential role in the thyroid hormone-dependent endocytosis of type II iodothyronine 5'-deiodinase. J Biol Chem 2000;275(41):31701-7.
19. Li G, Rungger-Brandle E, Just I, Jonas JC, Aktories K, Wollheim CB. Effect of disruption of actin filaments by Clostridium botulinum C2 toxin on insulin secretion in HIT-T15 cells and pancreatic islets. Mol Biol Cell 1994;5(11):1199-213.
20. Lang T, Wacker I, Wunderlich I, Rohrbach A, Giese G, Soldati T, et al. Role of actin cortex in the subplasmalemmal transport of secretory granules in PC-12 cells. Biophys J 2000;78(6):2863-77.
21. Olofsson CS, Gopel SO, Barg S, Galvanovskis J, Ma X, Salehi A, et al. Fast insulin secretion reflects exocytosis of docked granules in mouse pancreatic B-cells. Pflugers Arch 2002;444(1-2):43-51.
22. Ohara-Imaizumi M, Nishiwaki C, Kikuta T, Nagai S, Nakamichi Y, Nagamatsu S. TIRF imaging of docking and fusion of single insulin granule motion in primary rat pancreatic beta-cells: different behaviour of granule motion between normal and Goto-Kakizaki diabetic rat beta-cells. Biochem J 2004;381(Pt 1):13-8.
23. Macdonald PE, Obermuller S, Vikman J, Galvanovskis J, Rorsman P, Eliasson L. Regulated Exocytosis and Kiss-and-Run of Synaptic-Like Microvesicles in INS-1 and Primary Rat {beta}-Cells. Diabetes 2005;54(3):736-43.
24. Desnos C, Schonn JS, Huet S, Tran VS, El-Amraoui A, Raposo G, et al. Rab27A and its effector MyRIP link secretory granules to F-actin and control their motion towards release sites. J Cell Biol 2003;163(3):559-70.
25. Fukuda M, Itoh T. Slac2-a/melanophilin contains multiple PEST-like sequences that are highly sensitive to proteolysis. J Biol Chem 2004;279(21):22314-21.
26. Suzuki K, Hata S, Kawabata Y, Sorimachi H. Structure, activation, and biology of calpain. Diabetes 2004;53 Suppl 1:S12-8.
27. Karcher RL, Roland JT, Zappacosta F, Huddleston MJ, Annan RS, Carr SA, et al. Cell cycle regulation of myosin-V by calcium/calmodulin-dependent protein kinase II. Science 2001;293(5533):1317-20.

28. Iida Y, Senda T, Matsukawa Y, Onoda K, Miyazaki JI, Sakaguchi H, et al. Myosin light-chain phosphorylation controls insulin secretion at a proximal step in the secretory cascade. Am J Physiol 1997;273(4 Pt 1):E782-9.
29. Casaletti L, Tauhata SB, Moreira JE, Larson RE. Myosin-Va proteolysis by Ca2+/calpain in depolarized nerve endings from rat brain. Biochem Biophys Res Commun 2003;308(1):159-64.
30. Asfari M, Janjic D, Meda P, Li G, Halban PA, Wollheim CB. Establishment of 2-mercaptoethanol-dependent differentiated insulin-secreting cell lines. Endocrinology 1992;130(1):167-78.
31. Merglen A, Theander S, Rubi B, Chaffard G, Wollheim CB, Maechler P. Glucose sensitivity and metabolism-secretion coupling studied during two-year continuous culture in INS-1E insulinoma cells. Endocrinology 2004;145(2):667-78.
32. Wick PF, Senter RA, Parsels LA, Uhler MD, Holz RW. Transient transfection studies of secretion in bovine chromaffin cells and PC12 cells. Generation of kainate-sensitive chromaffin cells. J Biol Chem 1993;268(15):10983-9.
33. Barg S, Olofsson CS, Schriever-Abeln J, Wendt A, Gebre-Medhin S, Renstrom E, et al. Delay between fusion pore opening and peptide release from large dense-core vesicles in neuroendocrine cells. Neuron 2002;33(2):287-99.

Figures:

FIG. 1. Disruption of the actin network accelerates insulin secretion.

a: Pheripheral localization of the actin network in INS-1 cells as demonstrated by Alexa Fluor 488-phalloidin stainings. The images represent the top (T), center (C) and bottom (B) sections of the cell. **b:** Capacitance increases (ΔC) under control conditions and after cytochalasin D (Cy D) treatment.

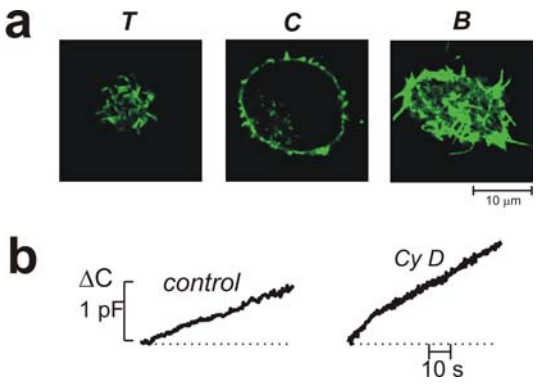

FIG. 2. Myosin 5a is expressed in INS-1E cells.

a: Immunoblot showing a band at 190 kDa representing myosin 5a (left lane). Protein ladder (L; right lane). **b:** Cofocal immunocytochemistry of myosin 5a in green (left panels), insulin in red (middle panels) and an overlay (right panels). The lower panel shows high magnification images of the selected region in the upper panel.

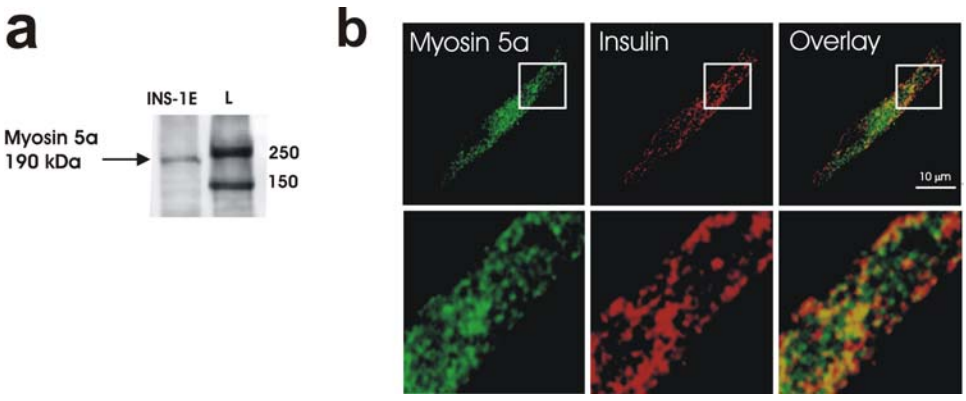

FIG. 3. Down-regulated expression of Myosin 5a by RNAinterference inhibits hormone secretion.

a: Expression of myosin 5a (top panel) and non-muscle myosin 2a (lower panel) in COS-7 cells co-transfected with a myosin 5a-expressing vector in combination with either silMyo5a1 for silencing of myosin 5a (RNAi Myosin 5a) or empty pSUPER (control). **b:** Growth hormone (GH) release (secreted/total content) under basal and stimulated (stim) conditions measured by ELISA. INS-1E cells were co-transfected with a vector expressing GH together with either silMyo5a1 for silencing of myosin 5a (RNAi Myosin 5a) or empty pSUPER (control).

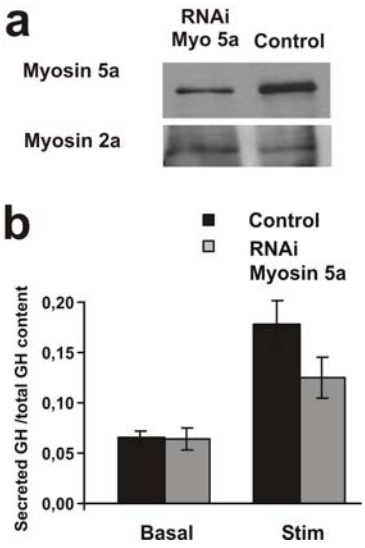

FIG. 4. Silencing of myosin 5a or Slac2c/ MYRIP results in similar inhibitory effects on exocytosis.

a: Capacitance increase (ΔC) in INS-1E cells transfected with pSuperEGFP (control) or SilMyo5a1-EGFP (RNAi Myosin5a). The left panel shows the average total ΔC during a train of depolarisations. The right panel shows representative capacitance traces from one control and one RNAi Myosin 5a

experiment in response to a train of ten depolarisating pulses (from 0 to –70 mV). **b:** As in (a) but cells were transfected with SilSlac-2c-EGFP (RNAi Slac-2c) instead. * p<0.05.

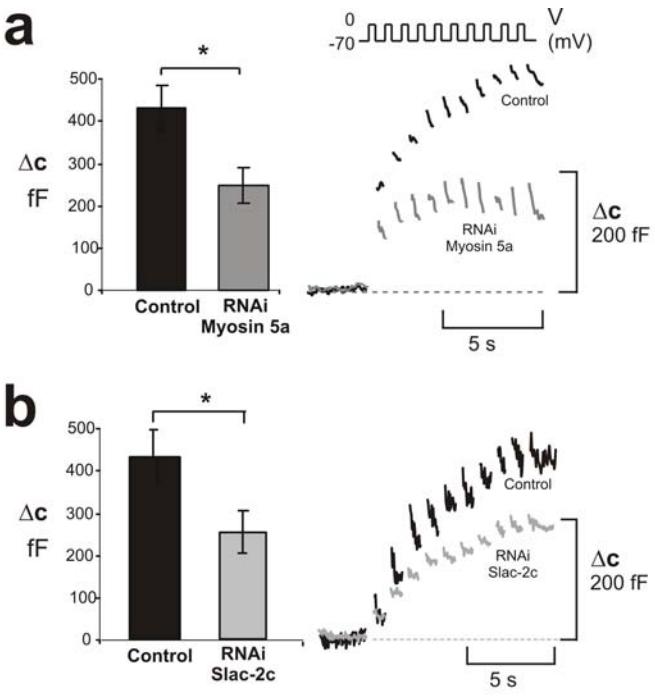

FIG. 5. Antibody inhibition of myosin 5a-cargo interaction results in use-dependent inhibition of exocytosis.

a: Capacitance increase (ΔC) in response to trains of ten depolarisating pulses from 0 to –70 mV applied at 2-6 minutes after whole-cell establishment. An antibody blocking the interaction between myosin 5a and Slac-2c/MYRIP was included in the intracellular pipette solution (light grey traces). Non immunized IgG was used as control (dark grey traces).

b: Average ΔC elicited by trains applied at 2-6 minutes. The black line represents the least squares fit to the first order exponential decay function.

c: Corresponding mean integrated Ca^{2+} currents (Q) elicited by the trains. p<0.05, ** p<0.01.

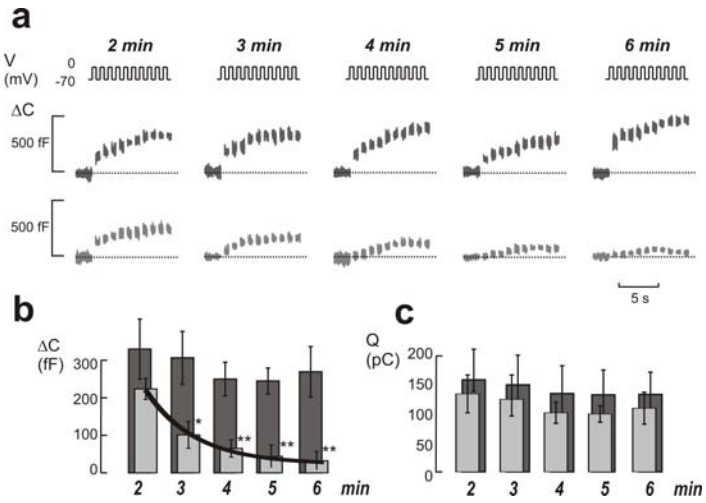

FIG. 6. Imaging of docked insulin granules by TIRF microscopy.

a: TIRF image of an INS-1E cell, transfected with a vector expressing IAPP-emerald, to visualize granules. **b:** INS-1E cells co-transfected with IAPP-emerald in combination with either silMyo5a1 (RNAi Myosin 5a) or empty pSuper (control). The figure shows the average number of docked granules in eight myosin 5a silencing (grey line) and control (black line) experiments during 20 minutes of glucose stimulation. Data are presented as the number of docked granules in every image correlated to the number of granules at the onset of experiment (ratio docked/initial number of docked granules). * $p<0.05$, ** $p<0.01$.